A&A 418, 703–715 (2004)
DOI: 10.1051/0004-6361:20035717

Astronomy & Astrophysics

Nitrogen abundances in planet-harbouring stars

A. Ecuvillon[1], G. Israelian[1], N. C. Santos[2,3], M. Mayor[3], R. J. García López[1,4], and S. Randich[5]

[1] Instituto de Astrofísica de Canarias, 38200 La Laguna, Tenerife, Spain
[2] Centro de Astronomia e Astrofisica de Universidade de Lisboa, Observatorio Astronomico de Lisboa, Tapada de Ajuda, 1349-018 Lisboa, Portugal
[3] Observatoire de Genève, 51 ch. des Maillettes, 1290 Sauverny, Switzerland
[4] Departamento de Astrofísica, Universidad de La Laguna, Av. Astrofísico Francisco Sánchez s/n, 38206 La Laguna, Tenerife, Spain
[5] INAF/Osservatorio Astrofisico di Arcetri, Largo Fermi 5, 50125 Firenze, Italy

Received 20 November 2003 / Accepted 4 February 2004

Abstract. We present a detailed spectroscopic analysis of nitrogen abundances in 91 solar-type stars, 66 with and 25 without known planetary mass companions. All comparison sample stars and 28 planet hosts were analysed by spectral synthesis of the near-UV NH band at 3360 Å observed at high resolution with the VLT/UVES, while the near-IR N I 7468 Å was measured in 31 objects. These two abundance indicators are in good agreement. We found that nitrogen abundance scales with that of iron in the metallicity range $-0.6 <$ [Fe/H] $< +0.4$ with the slope 1.08 ± 0.05. Our results show that the bulk of nitrogen production at high metallicities was coupled with iron. We found that the nitrogen abundance distribution in stars with exoplanets is the high [Fe/H] extension of the curve traced by the comparison sample of stars with no known planets. A comparison of our nitrogen abundances with those available in the literature shows a good agreement.

Key words. stars: abundances – stars: chemically peculiar – stars: evolution – stars: planetary systems – Galaxy: solar neighbourhood

1. Introduction

Knowledge of CNO abundances in main sequence stars is clearly important because of the key role of the former in the chain of nucleosynthesis. They can give us information about the history of element production in different types of stars. Solar-type stars can be very informative as tracers of the chemical and dynamical evolution of the Galaxy (e.g. Pagel & Edmunds 1981; Edvardsson et al. 1993; Bensby et al. 2003) as they spend between 10^9 to several times 10^{10} years on the main sequence.

The abundant isotope ^{14}N is synthesized through the CNO cycles in a hydrogen-burning shell of the stellar interior. With regard to the chemistry of planet-harbouring stars, the study of the nitrogen abundances of solar-type dwarfs with and without known planets represents an important key to checking the "self-enrichment" scenario. This hypothesis attributes the origin of the overabundance of metals to the accretion of large amounts of metal-rich, H- and He-depleted rocky planetesimal materials onto the star.

On the one hand, in studying chemical abundances and planetary orbital parameters, several authors reject the possibility of pollution as the main source of the metallicity enhancement observed in planet host stars and propose instead that the metal-rich nature of stars with planets has most probably a "primordial" source in the high metallicity of the primordial cloud (Santos et al. 2001, 2002, 2003). The effect on metal abundances of contamination in the outer convective zone by accreted planetary material in FGK main sequence stars has been discussed in Pinsonneault et al. (2001) and the same conclusion was reached. However, the possibility that pollution may occur has not been excluded. Israelian et al. (2001, 2003) have found evidence of the infall of a planet into the planet host star HD 82943. ^{6}Li and ^{7}Li may provide an independent test to confirm this scenario (Israelian et al. 2003, 2004).

On the other hand, the "self-enrichment" scenario would imply that volatile element (with low condensation temperature T_C) abundances do not show overabundance in the same way that refractories do, since the elements of the former group are deficient in accreted materials relative to the latter. This hypothesis has to be tested by searching for possible differences among volatile elements, such as CNO, S and Zn, and refractory ones, such as α-elements Si, Mg, Ca, Ti and the iron-group elements. Smith et al. (2001) found out that a small subset of stars with planets bore this accretion signature. They discovered that these stars exhibit a trend of increasing [X/H] with increasing T_C for a given element X. However, a following study by Takeda et al. (2001) showed that all the elements, volatiles

Send offprint requests to: A. Ecuvillon,
e-mail: aecuvill@ll.iac.es

and refractories alike, of fourteen planet-harbouring stars behave quite similarly, suggesting that the enhanced metallicity is not caused by the accretion of rocky material but is rather of primordial origin. Recently, Sadakane et al. (2002) confirmed this result for nineteen elements, volatiles and refractories, in twelve planet host stars. Gonzalez et al. (2001) and Santos et al. (2000) did not find significant differences in the [C/Fe] and [O/Fe] values among planet-harbouring and field stars. Some of these authors derived nitrogen abundances from atomic lines (e.g. Gonzalez & Laws 2000; Gonzalez et al. 2001; Takeda et al. 2001; Sadakane et al. 2002). We note that most of them made no mention of their final results and conclusions concerning nitrogen.

Various studies have accumulated evidence that the production of nitrogen at low [Fe/H] proceeds principally as a primary rather than a secondary process (Pagel & Edmunds 1981; Bessel & Norris 1982; Carbon et al. 1987; Henry et al. 2000). The secondary process dominates at high metallicities. Two possible primary sources of nitrogen have been proposed. The first is intermediate mass (4–8 $M_{\odot}$) stars during their thermally pulsing asymptotic giant branch phases: if temperature conditions are suitable, primary nitrogen can be produced by CN-processing in the convective envelope from freshly synthesized dredged up carbon (Marigo 2001; van den Hoek & Groenewegen 1997). The second source is rotating massive stars (Maeder & Meynet 2000). The latter would imply uncoupled N and Fe abundances and a nitrogen overproduction relative to iron.

Recently, Liang et al. (2001) and Pettini et al. (2002) concluded that the contribution by massive stars to the nitrogen abundance is generally very low, and that the dominant N contributors are intermediate and low mass stars (ILMS). Although the nitrogen is chiefly primary at low [Fe/H], ILMS are also sources of secondary nitrogen. The relative weights of the secondary and primary components depend on the interplay between secondary enrichment caused by dredge-up episodes and the primary contribution given by the CNO cycle during the envelope burning. Shi et al. (2002) obtained similar results by measuring N I lines in a large sample of disk stars with a metallicity range of $-1.0 < [\mathrm{Fe/H}] < +0.2$.

However, the situation is rather confused. Other authors support the origin of primary nitrogen in massive stars (e.g. Izotov & Thuan 2000) because of the low scatter of [N/O] ratios in galaxies observed at different stages of their evolution, which would imply no time delay between the injection of nitrogen and oxygen. Meynet & Maeder (2002) have discussed the effect of rotation in the production of primary and secondary nitrogen in intermediate and high mass stars, introducing axial rotation and rotationally induced mixing of chemical species in their stellar models. They concluded that ILMS are the main source of primary nitrogen at low metallicities.

The main problem that has traditionally made it difficult to measure nitrogen abundances is that there are very few atomic nitrogen lines in the red part of the spectrum. Efficient modern detectors now enable us to obtain high-resolution near-UV spectra, which allows us to carry out a precise and independent study of nitrogen abundance by using the NH band at 3360 Å.

The purpose of this work is to obtain a systematic, uniform and detailed study of nitrogen abundance in two samples of solar-type dwarfs, a large set of planet hosts and a comparison volume-limited sample of stars with no known planetary mass companions. We used two independent indicators in the abundance determination: spectral synthesis of the NH band in near-UV high-resolution spectra and the near-IR N I 7468 Å line.

2. Observations

Spectra for most of the planet-harbouring stars have been collected and used to derive precise stellar parameters in a series of recent papers (e.g. Santos et al. 2001, 2003, 2004). For measurement of the N I 7468 Å line we used all the spectra of this set obtained with the FEROS spectrograph on the 2.2 m ESO/MPI telescope (La Silla, Chile), the SARG spectrograph on the 3.5 m TNG and the UES spectrograph on the 4.2 m WHT (both at the Roque de los Muchachos Observatory, La Palma), and other spectra from subsequent observational runs using the same instruments.

For NH band synthesis, we used the same spectra as those in Santos et al. (2002) to derive beryllium abundances[1]. New spectra were obtained with the UVES spectrograph, at the VLT/UT2 Kueyen telescope (Paranal Observatory, ESO, Chile)[2]. The observing log for the spectra from campaigns carried out after Santos et al. (2002) and Bodaghee et al. (2003) are listed in Tables 1 and 2. The obtained high S/N spectra have a minimum resolution $R \geq 50\,000$.

The data reduction for the SARG and UVES spectra was done using IRAF tools in the `echelle` package. Standard background correction, flatfield and extraction procedures were used. The wavelength calibration was performed using a ThAr lamp spectrum taken on the same night. The FEROS spectra were reduced using the FEROS pipeline software.

3. Analysis

Abundances for all elements were determined using a standard local thermodynamic equilibrium (LTE) analysis with the revised version of the spectral synthesis code MOOG (Sneden 1973) and a grid of Kurucz (1993) ATLAS9 atmospheres. All the atmospheric parameters, $T_{\rm eff}$, $\log g$, ξ_t and [Fe/H], and the corresponding uncertainties were taken from Santos et al. (2004). The adopted solar abundances for nitrogen and iron were $\log \epsilon(\mathrm{N})_{\odot} = 8.05$ dex (Anders & Grevesse 1989) and $\log \epsilon(\mathrm{Fe})_{\odot} = 7.47$ dex (Santos et al. 2004).

3.1. Synthesis of NH band

The NH molecular feature is the strongest one in the spectral region $\lambda\lambda$3345–3375 Å. We determined nitrogen abundances by fitting synthetic spectra to data in this wavelength range. The NH spectra were calculated with the dissociation potential $D_0(\mathrm{NH}) = 3.37 \pm 0.06$ eV recommended in Grevesse et al. (1990).

[1] Observing run 66.C-0116A.
[2] Observing run 68.C-0058A.

Table 1. Observing log for the new set of stars with planets and brown dwarf companions. Near-UV and optical spectra were obtained with UVES, and with SARG and FEROS, respectively. The *S/N* ratio is provided at 3357 Å for near-UV data and at 7400 Å in optical spectra.

Star	V	Obser. Run	*S/N*	Date
HD 6434	7.7	UVES	150	Oct. 2001
HD 22049	3.7	UVES	150	Oct. 2001
HD 30177	8.4	FEROS	200	Mar. 2003
HD 40979	6.8	SARG	220	Oct. 2003
HD 46375	7.8	UVES	150	Nov. 2001
HD 65216	9.6	FEROS	250	Mar. 2003
HD 68988	8.2	SARG	160	Oct. 2003
HD 72659	7.4	FEROS	200	Mar. 2003
HD 73256	8.1	FEROS	200	Mar. 2003
HD 73526	9.0	FEROS	250	Mar. 2003
HD 76700	8.1	FEROS	200	Mar. 2003
HD 83443	8.2	UVES	120	Nov. 2001
HD 10647	5.5	UVES	160	Oct. 2001
HD 142415	7.3	FEROS	250	Mar. 2003
HD 169830	5.9	UVES	160	Oct. 2001
HD 178911B	6.7	SARG	280	Oct. 2003
HD 179949	6.3	UVES	160	Oct. 2001
HD 202206	8.1	UVES	150	Nov. 2001
HD 209458	7.7	UVES	150	Nov. 2001
HD 216770	8.1	SARG	220	Oct. 2003
HD 219542B	8.2	SARG	230	Oct. 2003
HD 222582	7.7	UVES	180	Nov. 2001

Table 2. Observing log for the new set of comparison stars (stars without known giant planets). Near-UV spectra are obtained with UVES. The *S/N* ratio is provided at 3357 Å.

Star	V	Obser. Run	*S/N*	Date
HD 4391	5.8	UVES	240	Oct. 2001
HD 7570	4.9	UVES	150	Oct. 2001
HD 10700	3.5	UVES	200	Oct. 2001
HD 14412	6.3	UVES	130	Oct. 2001
HD 20010	3.9	UVES	240	Oct. 2001
HD 20766	5.5	UVES	140	Oct. 2001
HD 20794	4.3	UVES	130	Oct. 2001
HD 20807	5.2	UVES	180	Oct. 2001
HD 23484	7.0	UVES	160	Oct. 2001
HD 30495	5.5	UVES	120	Oct. 2001
HD 36435	7.0	UVES	110	Oct. 2001
HD 38858	6.0	UVES	80	Oct. 2001
HD 43162	6.4	UVES	180	Nov. 2001
HD 43834	5.1	UVES	180	Nov. 2001
HD 69830	5.9	UVES	130	Oct. 2001
HD 72673	6.4	UVES	110	Nov. 2001
HD 76151	6.0	UVES	90	Oct. 2001
HD 84117	4.9	UVES	200	Nov. 2001
HD 189567	6.1	UVES	140	Oct. 2001
HD 192310	5.7	UVES	90	Oct. 2001
HD 211415	5.3	UVES	120	Oct. 2001

A detailed line list from Yakovina & Pavlenko (1998) was adopted. These authors obtained a good fit to the Kurucz Solar Atlas (Kurucz et al. 1984) by changing oscillator strength values of the strongest lines and continuum level in a list of atomic and molecular lines from Kurucz's 1993 database. In our analysis, we slightly modified $\log gf$ values of this line list[3] (changes smaller than 0.01 dex in most cases) in order to avoid modifying the continuum level when fitting the high-resolution Kurucz Solar Atlas (Kurucz et al. 1984) with a solar model having $T_{\rm eff}$ = 5777 K, $\log g$ = 4.44 dex and ξ_t = 1.0 km s^{-1}, assuming the solar N abundance of $\log \epsilon\,(\mathrm{N})_\odot = 8.05$ dex.

All our targets are solar-type dwarfs with [Fe/H] values between −0.6 and +0.4 dex and $T_{\rm eff}$ between 5000 and 6300 K. Stars with lower $T_{\rm eff}$ were rejected since they would have introduced great uncertainties in the abundance results. The discarded targets were HD 27442, HD 192263, HD 74576 and HD 23484, with $T_{\rm eff}$ of 4825 K, 4947 K, 5000 K and 5176 K, respectively.

The main difficulties were the severe atomic line contamination of the NH features and the crowding of the lines in the UV region. The oscillator strengths of these lines are not known with high accuracy. The crowding of blended lines worsens with the increase of metallicity. This characteristic involves difficulties when fixing the continuum level since the whole spectral region is depressed by line absorption. The continuum was normalized with 5th order polynomia using the CONT task of IRAF. However we could make further improvements in the placement of the continuum using the Kurucz Solar Flux Atlas (Kurucz et al. 1984) and DIPSO task of the STARLINK software: the continuum level was determined by superimposing observed and synthetic solar spectra and selecting some points of reference. Figure 1 shows significant points in continuum determination, selected in the spectral regions $\lambda\lambda$3344–3350 Å, $\lambda\lambda$3350–3358 Å and $\lambda\lambda$3362–3370 Å for HD 17051. This method was valid for stars with $T_{\rm eff}$ and metallicities around solar values, while in cooler objects we were not able to assure that the continuum level could be scaled to the Sun.

In order to find the best synthetic spectrum for each star, we used the program FITTING. This program allows us to create a grid of synthetic spectra for several free parameters, such as abundances, atmospheric parameters, metallicity, etc., and to compare it with the observed spectrum. To generate synthetic spectra, it calls the spectral synthesis code MOOG. The best

[3] The full line list is available in `www.iac.es`

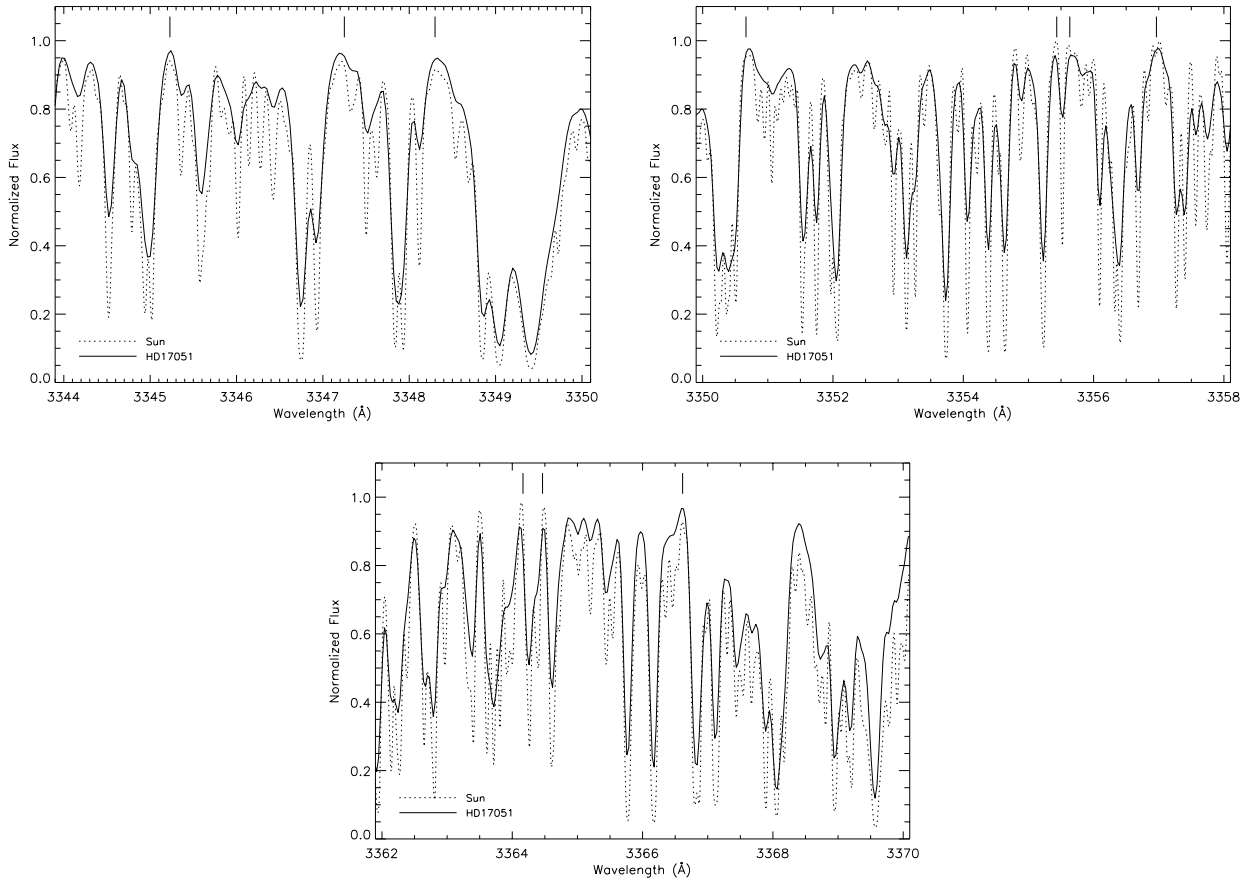

Fig. 1. HD 17051 and solar spectra in the regions $\lambda\lambda$3344–3350 Å, $\lambda\lambda$3350–3358 Å and $\lambda\lambda$3362–3370 Å. Vertical lines represent points of reference in continuum determination.

fit is determined by applying a χ^2 minimization method to the spectral regions considered to be the most significant.

We used a Gaussian function with a *FWHM* of 0.07 Å for the instrumental broadening, and a rotational broadening function with $v \sin i$ = 4 km s^{-1}. No macroturbulence broadening was used. We assumed the same rotational velocity for all the targets since small differences would affect only χ^2 values, not final nitrogen abundances. Only for HD 120136 and HD 19994 we did take $v \sin i$ = 14.5 km s^{-1} and $v \sin i$ = 8.2 km s^{-1} from the CORALIE database. We stress that planet searches based on the Doppler technique are biased in favour of old stars with low $v \sin i$ and therefore all our targets are slow rotators. In any case, precise values of $v \sin i$ are not required for the abundance analysis since it is well known that the rotational convolution is not affecting the *EW* of the line (Gray 1992). Our test with χ^2 analysis confirms this assumption for the stars considered in our study. In the estimate of damping constants, the Unsold aproximation was adopted for all atomic and molecular lines. We have verified that the damping effects do not affect our final abundances.

At first, the abundances of all relevant elements were fitted for a set of stars with different atmospheric parameters. Next, the same fits were performed by scaling the abundance of elements other than nitrogen to the [Fe/H] value and by changing only the nitrogen abundance. The same results were obtained in both cases, therefore all the following fittings were carried out by scaling elements other than nitrogen to iron.

The program FITTING introduced the following data in the code MOOG: the atmospheric model, the line list and the range of nitrogen abundance of the grid of synthetic spectra. Then χ^2 values were calculated by comparing each synthetic spectrum with the observed one in the following spectral regions: $\lambda\lambda$3344.0–3344.7 Å, $\lambda\lambda$3345.9–3346.9 Å, $\lambda\lambda$3347.2–3348.2 Å, $\lambda\lambda$3353.5–3354.5 Å, $\lambda\lambda$3357.0–3358.0 Å, $\lambda\lambda$3358.5–3359.0 Å, $\lambda\lambda$3361.8–3362.5 Å, $\lambda\lambda$3363.0–3363.75 Å, $\lambda\lambda$3363.8–3365.5 Å, $\lambda\lambda$3368.0–3368.8 Å, $\lambda\lambda$3369.1–3369.9 Å, $\lambda\lambda$3371.8–3372.8 Å and $\lambda\lambda$3374.8–3376.0 Å. $\chi^2_{\rm tot}$ was the sum of χ^2 values[4] of the mentioned spectral regions. The nitrogen abundance corresponding to minimum $\chi^2_{\rm tot}$ value was extracted and listed in Tables 4 and 5. The fact that $\chi^2_{\rm tot}$ is smaller for high $T_{\rm eff}$ can be understood as the consequence of a suitable placement of the continuum in stars more similar to the Sun.

Figure 2 shows fits for a short, significant spectral region. The observed solar spectrum from the Kurucz Solar Atlas (Kurucz et al. 1984) and the synthetic spectrum are represented in the left panel. The case of the planet host star HD 17051 is

[4] $\chi^2 = \sum_{i=1}^{N} (F_i - S_i)^2$, where F_i and S_i are the observed and synthetic spectra fluxes, respectively, at the wavelength i.

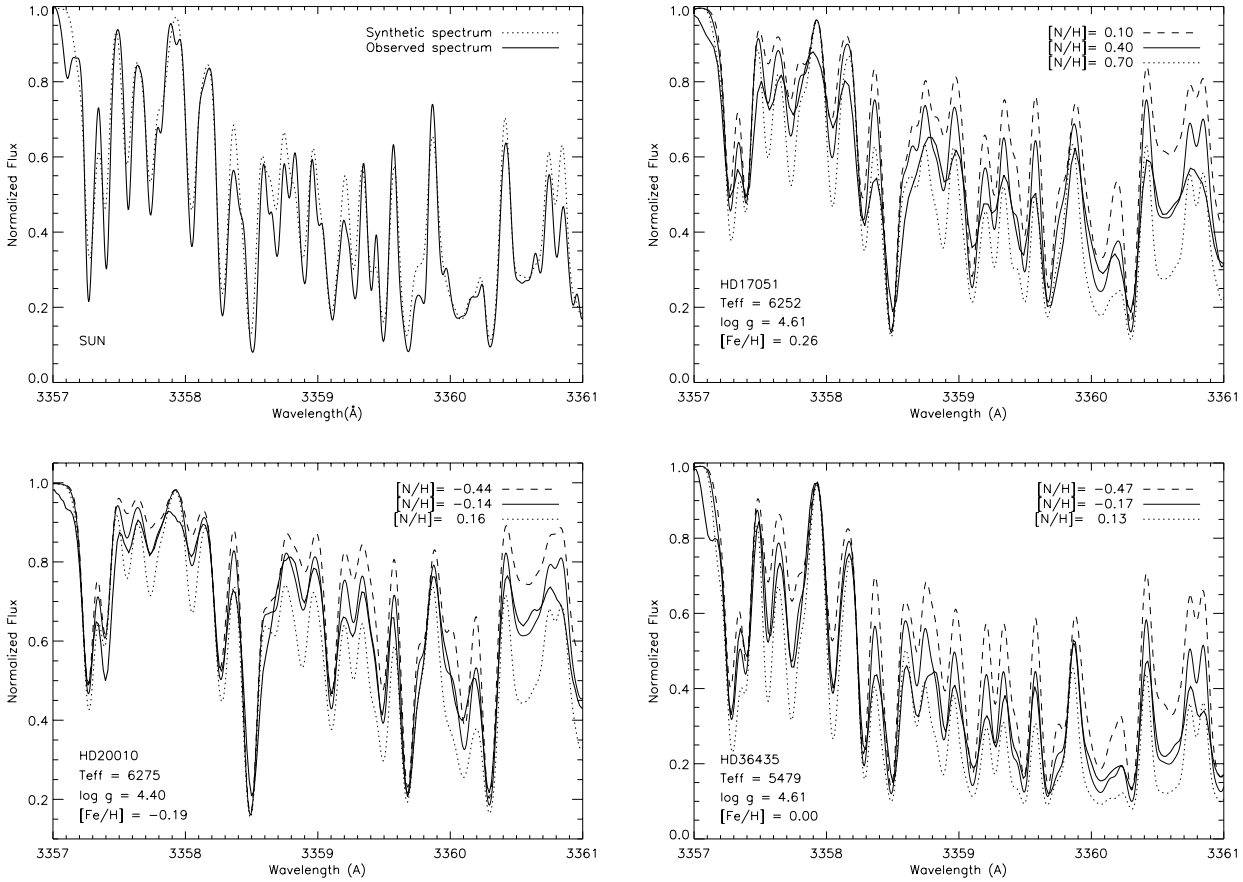

Fig. 2. *Top left*: solar observed (solid line) and synthetic (dotted line) spectra in the spectral region $\lambda\lambda$3357–3361 Å. *Top right and bottom*: observed spectrum (thick solid line) and three synthetic spectra (dotted, dashed and solid lines) for different values of [N/H], for three targets.

Table 3. Sensitivity of the nitrogen abundance, derived from the NH band at 3360 Å and from the N I line at 7468 Å, to changes of 100 K in effective temperature, 0.2 dex in gravity and 0.2 dex in metallicity.

	Star	HD 46375	HD 73526	HD 7570
	($T_{\rm eff}$; log g; [Fe/H])	(5268; 4.41; 0.20)	(5699; 4.27; 0.27)	(6140; 4.39; 0.18)
NH:	$\Delta T_{\rm eff}$ = ±100 K	±0.09	±0.09	±0.09
N I:	$\Delta T_{\rm eff}$ = ±100 K	∓0.11	∓0.08	∓0.07

	Star	HD 19994	HD 12661	HD 142415
	($T_{\rm eff}$; log g; [Fe/H])	(6190; 4.19; 0.24)	(5702; 4.33; 0.36)	(6045; 4.53; 0.21)
NH:	$\Delta \log g$ = ±0.2 dex	∓0.04	∓0.05	∓0.05
N I:	$\Delta \log g$ = ±0.2 dex	±0.06	±0.06	±0.06

	Star	HD 143761	HD 187123	HD 76700
	($T_{\rm eff}$; log g; [Fe/H])	(5853; 4.41; −0.20)	(5845; 4.42; 0.13)	(5737; 4.25; 0.41)
NH:	Δ([Fe/H]) = ±0.2 dex	±0.14	±0.17	±0.18
N I:	Δ([Fe/H]) = ±0.2 dex	∓0.03	∓0.03	∓0.03

represented in the right panel (the observed spectrum and three synthetic spectra for different values of nitrogen abundance).

Uncertainties in the atmospheric parameters are of the order of 50 K in $T_{\rm eff}$, 0.12 dex in log g, 0.08 km s^{-1} in the microturbulence and 0.05 dex in the metallicity (see Santos et al. 2004). To know how variations in the atmospheric parameters affect NH abundances, for each parameter a set of three stars having very different parameter values was selected. For each set of stars we then tested [N/H] sensitivity to changes in the parameter (±100 K in the case of $T_{\rm eff}$, ±0.2 dex in log g

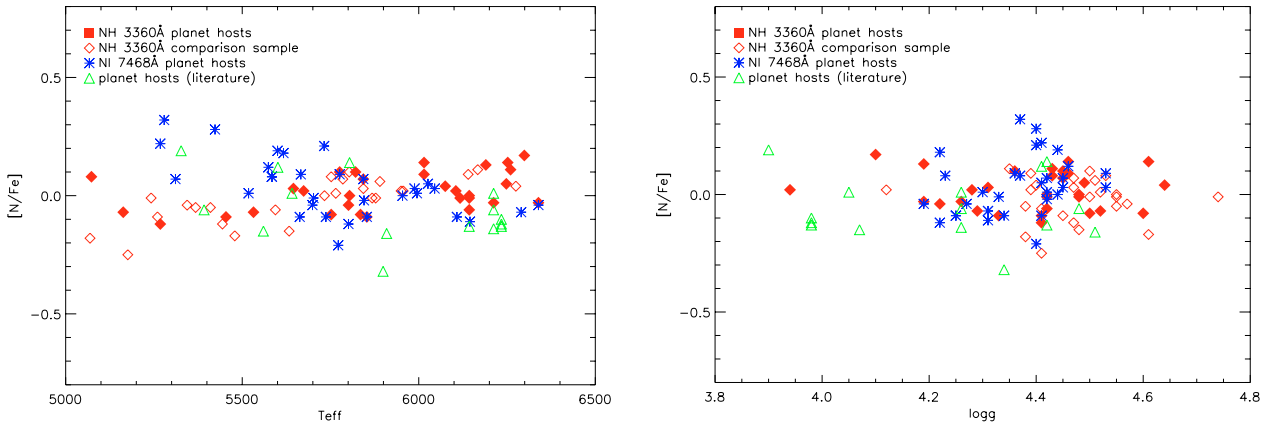

Fig. 3. [N/Fe] vs. $T_{\rm eff}$ and $\log g$. Filled and open diamonds represent planet host and comparison sample stars from NH band synthesis, respectively. Asterisks and open triangles denote planet host stars from N I line and from literature values, respectively.

and [Fe/H], and 0.3 km s^{-1} in ξ_t). The results are shown in Table 3. No microturbolence effects were included, since an increase of 0.3 km s^{-1} produced an average decrease of 0.003 dex in nitrogen abundances, which is negligible with regard to the effects of other parameters. The sensitivity of the NH abundance was applied in the propagation of each parameter error on abundances. Also, a continuum uncertainty effect of the order of 0.1 dex was considered. All effects were added quadratically to obtain the final uncertainties for the nitrogen abundances.

3.2. The N I absorption at 7468.27 Å

Nitrogen abundance analysis based on the feature at 7468.27 Å was carried out diferentially with respect to the Sun. Wavelength and excitation energies of the lower level were taken from Moore et al. (1966) and a solar gf value ($\log gf = -0.15$) was computed using equivalent width measured in the Kurucz Solar Atlas (Kurucz et al. 1984) (4.2 mÅ) and a solar model with $T_{\rm eff} = 5777$ K, $\log g = 4.44$ dex and $\xi_t = 1.0$ km s^{-1}, assuming the solar N abundance of $\log \epsilon(\mathrm{N})_\odot = 8.05$ dex. Equivalent widths in the observed stars were determined by Gaussian fitting using the SPLOT task of IRAF, and abundances were computed using the ABFIND driver of MOOG.

The high resolution spectra we used provided us with very reliable measurements in most cases. However, a strong fringing effect around 7468 Å prevented us from measuring high precision EW values in some cases; therefore, the corresponding EW uncertainties are higher.

The sensitivity of the N I line to variations in atmospheric parameters was estimated in the same way as in the NH case (see Sect. 3.1). The results are shown in Table 3. To take into account inaccuracies caused by the continuum determination, equivalent widths for the highest and the lowest continuum levels were measured, and the corresponding abundance errors were added in quadrature to the abundance uncertainties derived from inaccuracies in the atmospheric parameters.

Dependences on $T_{\rm eff}$ and on $\log g$ of [N/Fe] derived by both methods are presented in Fig. 3. We note that no characteristic trends appear in either case. This means that our results are almost free from systematic errors.

4. Nitrogen abundances from near-UV spectra

In the literature there are already a few studies that use the NH band at 3360 Å to determine nitrogen abundances by spectral synthesis, but only for metal-poor dwarfs (Bessel & Norris 1982; Tomkin & Lambert 1984; Laird 1985; Carbon et al. 1987).

We analysed near-UV high-resolution spectra of 28 planet host stars and 25 comparison sample stars with the goal of checking for possible differences in nitrogen abundances between both samples. All the results for planet host and comparison sample stars are presented in Tables 4 and 5, respectively.

Figure 4 shows the [N/H] and [N/Fe] abundance ratios as functions of [Fe/H] for these two samples. These plots indicate that the abundance trend for stars with planets is almost indistinguishable from that of the comparison stars. Because of the iron enhancement that planet-harbouring stars present, their abundance distributions are the high [Fe/H] extensions of the curves traced by the comparison sample stars. No peculiar behaviour of the nitrogen abundance seems to be associated with the presence of planets.

On the whole, the [N/Fe] vs. [Fe/H] trend appears to be almost flat, since the slope value is 0.10 ± 0.05. Nevertheless, a small trend to increase with [Fe/H] cannot be excluded. The [N/H] vs. [Fe/H] plot shows that the behaviour of the N abundance is not significantly different from that of Fe; the two elements keep pace with each other. Moreover, no significant nitrogen overproduction relative to iron is observed.

The [N/H] distributions for both samples are represented in Fig. 5 (upper panel). An interesting feature of the histogram is that the planet-harbouring stars set does not present a symmetrical distribution, as the comparison sample does. The distribution increases for increasing [N/H] values until reaching the highest value, not centred on the [N/H] range. However, this peculiarity could be caused by the lack of objects with metallicities higher than 0.5 dex. Santos et al. (2001, 2003, 2004) found a similar shape in the iron distribution.

Table 4. Nitrogen abundances from NH band synthesis for a set of stars with planets and brown dwarf companions. Last column lists $\chi^2_{\rm tot}$ values.

Star	$T_{\rm eff}$ (K)	$\log g$ (cm s^{-2})	ξ_t (km s^{-1})	[Fe/H]	[N/H]	$\chi^2_{\rm tot}$
HD 6434	5835 ± 50	4.60 ± 0.15	1.53 ± 0.10	−0.52 ± 0.05	−0.60 ± 0.13	10.13
HD 9826	6212 ± 64	4.26 ± 0.13	1.69 ± 0.16	0.13 ± 0.08	0.10 ± 0.14	6.27
HD 13445	5163 ± 37	4.52 ± 0.13	0.72 ± 0.06	−0.24 ± 0.05	−0.31 ± 0.10	7.27
HD 16141	5801 ± 30	4.22 ± 0.12	1.34 ± 0.04	0.15 ± 0.04	0.11 ± 0.11	5.16
HD 17051	6252 ± 53	4.61 ± 0.16	1.18 ± 0.10	0.26 ± 0.06	0.40 ± 0.13	2.95
HD 19994	6190 ± 57	4.19 ± 0.13	1.54 ± 0.13	0.24 ± 0.07	0.37 ± 0.10	5.27
HD 22049	5073 ± 42	4.43 ± 0.08	1.05 ± 0.06	−0.13 ± 0.04	−0.05 ± 0.12	27.88
HD 38529	5674 ± 40	3.94 ± 0.12	1.38 ± 0.05	0.40 ± 0.06	0.42 ± 0.12	13.43
HD 46375	5268 ± 55	4.41 ± 0.16	0.97 ± 0.06	0.20 ± 0.06	0.07 ± 0.13	19.76
HD 52265	6103 ± 52	4.28 ± 0.15	1.36 ± 0.09	0.23 ± 0.07	0.25 ± 0.10	3.10
HD 75289	6143 ± 53	4.42 ± 0.13	1.53 ± 0.09	0.28 ± 0.07	0.21 ± 0.13	3.43
HD 82943	6016 ± 30	4.46 ± 0.08	1.13 ± 0.04	0.30 ± 0.04	0.39 ± 0.10	6.68
HD 83443	5454 ± 61	4.33 ± 0.17	1.08 ± 0.08	0.35 ± 0.08	0.26 ± 0.14	21.82
HD 92788	5821 ± 41	4.45 ± 0.06	1.16 ± 0.05	0.32 ± 0.05	0.42 ± 0.12	12.27
HD 10647	6143 ± 31	4.48 ± 0.08	1.40 ± 0.08	−0.03 ± 0.04	−0.03 ± 0.11	3.43
HD 108147	6248 ± 42	4.49 ± 0.16	1.35 ± 0.08	0.20 ± 0.05	0.25 ± 0.12	5.58
HD 120136	6339 ± 73	4.19 ± 0.10	1.70 ± 0.16	0.23 ± 0.07	0.20 ± 0.14	1.87
HD 121504	6075 ± 40	4.64 ± 0.12	1.31 ± 0.07	0.16 ± 0.05	0.20 ± 0.12	7.71
HD 134987	5776 ± 29	4.36 ± 0.07	1.09 ± 0.04	0.30 ± 0.04	0.40 ± 0.11	11.96
HD 143761	5853 ± 25	4.41 ± 0.15	1.35 ± 0.07	−0.21 ± 0.04	−0.30 ± 0.11	12.88
HD 169830	6299 ± 41	4.10 ± 0.02	1.42 ± 0.09	0.21 ± 0.05	0.38 ± 0.12	7.31
HD 179949	6260 ± 43	4.43 ± 0.05	1.41 ± 0.09	0.22 ± 0.05	0.33 ± 0.12	5.72
HD 202206	5752 ± 53	4.50 ± 0.09	1.01 ± 0.06	0.35 ± 0.06	0.27 ± 0.13	14.31
HD 209458	6117 ± 26	4.48 ± 0.08	1.40 ± 0.06	0.02 ± 0.03	0.01 ± 0.11	5.66
HD 210277	5532 ± 28	4.29 ± 0.09	1.04 ± 0.03	0.19 ± 0.04	0.12 ± 0.10	9.14
HD 217014	5804 ± 36	4.42 ± 0.07	1.20 ± 0.05	0.20 ± 0.05	0.20 ± 0.11	10.19
HD 217107	5646 ± 34	4.31 ± 0.10	1.06 ± 0.04	0.37 ± 0.05	0.40 ± 0.10	10.99
HD 222582	5843 ± 38	4.45 ± 0.07	1.03 ± 0.06	0.05 ± 0.05	0.12 ± 0.11	10.25

5. Nitrogen abundances from the N I 7468 Å line

Several studies of nitrogen abundances in metal-rich dwarfs with planets using near-IR N I lines have been published, but data for only a small number of planet host stars have been employed (fourteen planet-harbouring stars in the most extensive case, in Takeda et al. 2001) and most of them do not even mention their nitrogen abundance results (Gonzalez & Laws 2000; Gonzalez et al. 2001; Sadakane et al. 2002). Only Takeda et al. (2001) have presented their nitrogen abundance results from the measurement of the N I line at 8683 Å, as well as abundance results for another four volatile elements (C, O, S and Zn). They did not observe the tendency predicted by the "self-enrichment" hypothesis ([X/H] < [Fe/H] for metal-enriched planet host stars), a weak inverse trend ([X/H] > [Fe/H]) even seemed to appear for N and S.

We obtained nitrogen abundances for 31 planet host stars by equivalent width measurements of the N I line at 7468 Å. All atmospheric parameters, EW values with uncertainties and abundance results are listed in Table 6. Figure 6 shows the [N/H] and [N/Fe] abundance ratios as functions of [Fe/H] for planet host stars, from NH band and N I line sets, and for comparison sample stars. In Fig. 5 (top lower panel), the [N/H] distributions are shown for both the planet host (with values from both indicators) and comparison star samples. In all the plots the added values follow the same behaviour as those resulting from NH band analysis. The previously commented trends (see Sect. 4) are confirmed.

6. Comparison of the near-UV and 7468 Å line results

Two independent analyses were carried out, using different indicators of nitrogen abundance. We managed thereby to extend our data sample, as well as to check the agreement between both methods and to test the strength of our results.

We had available to us two different sets of data. The first consisted of near-UV spectra of planet host and comparison sample stars. The other was composed of optical and near-IR spectra of stars with planets. The comparison between the results of both indicators was performed using the eight targets that both sets had in common.

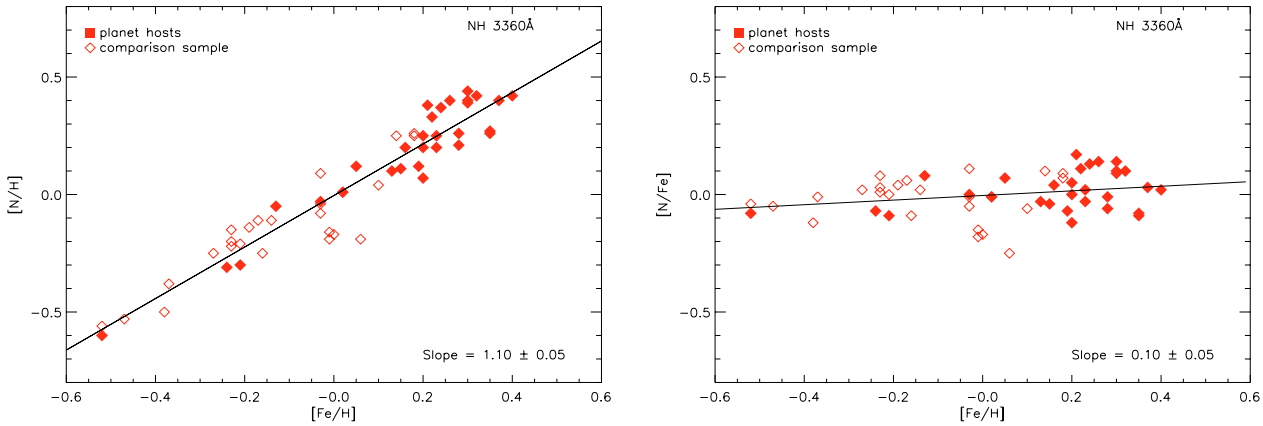

Fig. 4. [N/H] and [N/Fe] vs. [Fe/H] plots from NH 3360 Å band synthesis. Filled and open diamonds represent planet host and comparison sample stars, respectively. Linear least-squares fits to both samples together are represented and slope values are written at the bottom of each plot.

Table 5. Nitrogen abundances from NH band synthesis for a set of comparison stars (without giant planets). Last column lists $\chi^2_{\rm tot}$ values.

Star	$T_{\rm eff}$ (K)	$\log g$ (cm s^{-2})	ξ_t (km s^{-1})	[Fe/H]	[N/H]	$\chi^2_{\rm tot}$
HD 1461	5785 ± 50	4.47 ± 0.15	1.00 ± 0.10	0.18 ± 0.05	0.25 ± 0.13	6.72
HD 1581	5956 ± 44	4.39 ± 0.13	1.07 ± 0.09	−0.14 ± 0.05	−0.11 ± 0.12	4.15
HD 3823	5950 ± 50	4.12 ± 0.15	1.00 ± 0.10	−0.27 ± 0.05	−0.25 ± 0.13	4.89
HD 4391	5878 ± 53	4.74 ± 0.15	1.13 ± 0.10	−0.03 ± 0.06	−0.04 ± 0.13	8.21
HD 7570	6140 ± 41	4.39 ± 0.16	1.50 ± 0.08	0.18 ± 0.05	0.26 ± 0.12	6.28
HD 10700	5344 ± 29	4.57 ± 0.09	0.91 ± 0.06	−0.52 ± 0.04	−0.56 ± 0.11	15.42
HD 14412	5368 ± 24	4.55 ± 0.05	0.88 ± 0.05	−0.47 ± 0.03	−0.53 ± 0.11	16.58
HD 20010	6275 ± 57	4.40 ± 0.37	2.41 ± 0.41	−0.19 ± 0.06	−0.14 ± 0.15	3.69
HD 20766	5733 ± 31	4.55 ± 0.10	1.09 ± 0.06	−0.21 ± 0.04	−0.21 ± 0.11	8.35
HD 20794	5444 ± 31	4.47 ± 0.07	0.98 ± 0.06	−0.38 ± 0.04	−0.50 ± 0.11	14.72
HD 20807	5843 ± 26	4.47 ± 0.10	1.17 ± 0.06	−0.23 ± 0.04	−0.20 ± 0.11	7.44
HD 23484	5176 ± 45	4.41 ± 0.17	1.03 ± 0.06	0.06 ± 0.05	−0.19 ± 0.12	16.86
HD 30495	5868 ± 30	4.55 ± 0.10	1.24 ± 0.05	0.02 ± 0.04	0.01 ± 0.11	7.86
HD 36435	5479 ± 37	4.61 ± 0.07	1.12 ± 0.05	−0.00 ± 0.05	−0.17 ± 0.11	8.82
HD 38858	5752 ± 32	4.53 ± 0.07	1.26 ± 0.07	−0.23 ± 0.05	−0.15 ± 0..11	10.46
HD 43162	5633 ± 35	4.48 ± 0.07	1.24 ± 0.05	−0.01 ± 0.04	−0.16 ± 0.11	6.93
HD 43834	5594 ± 36	4.41 ± 0.09	1.05 ± 0.04	0.10 ± 0.05	0.04 ± 0.11	11.53
HD 69830	5410 ± 26	4.38 ± 0.07	0.89 ± 0.03	−0.03 ± 0.04	−0.08 ± 0.11	15.02
HD 72673	5242 ± 28	4.50 ± 0.09	0.69 ± 0.05	−0.37 ± 0.04	−0.38 ± 0.11	16.37
HD 76151	5803 ± 29	4.50 ± 0.08	1.02 ± 0.04	0.14 ± 0.04	0.25 ± 0.11	12.54
HD 84117	6167 ± 37	4.35 ± 0.10	1.42 ± 0.09	−0.03 ± 0.05	0.09 ± 0.12	4.16
HD 189567	5765 ± 24	4.52 ± 0.05	1.22 ± 0.05	−0.23 ± 0.04	−0.22 ± 0.11	9.65
HD 192310	5069 ± 49	4.38 ± 0.19	0.79 ± 0.07	−0.01 ± 0.05	−0.19 ± 0.13	19.83
HD 211415	5890 ± 30	4.51 ± 0.07	1.12 ± 0.07	−0.17 ± 0.04	−0.11 ± 0.11	7.88
HD 222335	5260 ± 41	4.45 ± 0.11	0.92 ± 0.06	−0.16 ± 0.05	−0.25 ± 0.12	12.98

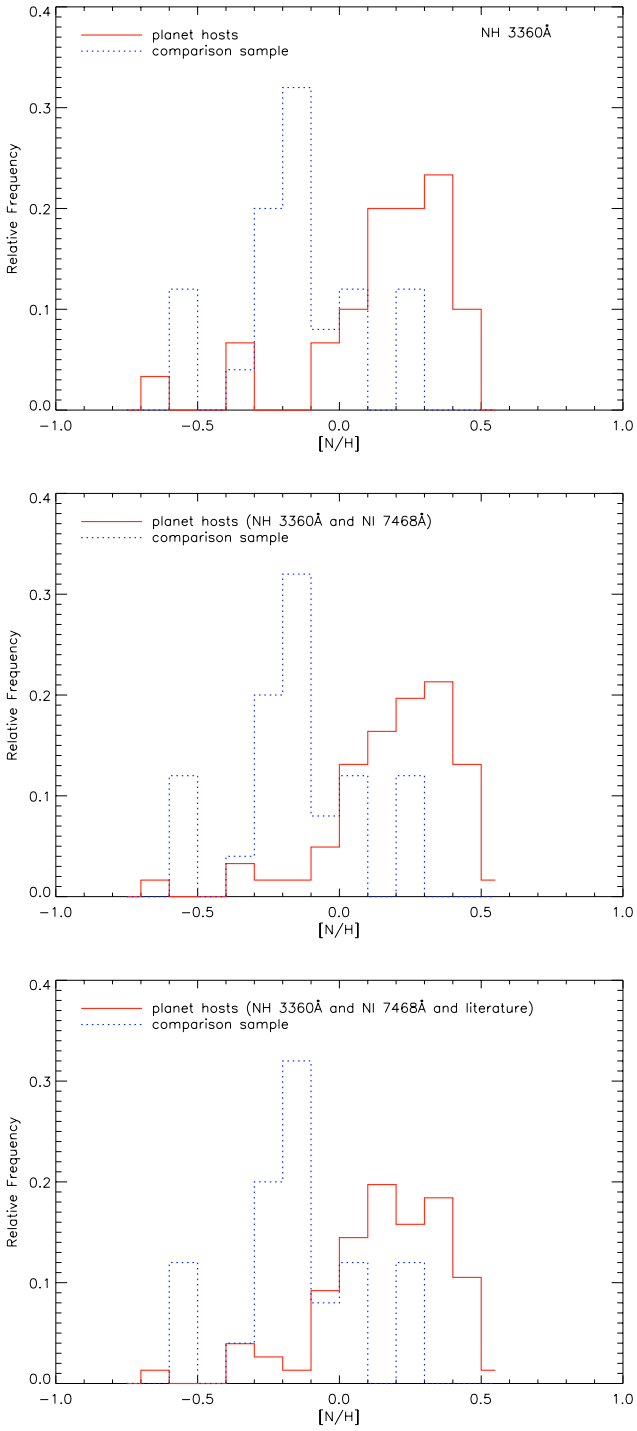

Fig. 5. [N/H] distributions, from NH band values (*upper panel*), from NH band and N I line values (*top lower panel*), and from NH band, N I line and literature values (*bottom panel*). Solid and dotted lines represent planet host and comparison sample stars, respectively.

Abundances resulting from both indicators are presented in Table 7. We stress the remarkable agreement in most cases. In the case of HD 19994 and HD 217107, both values fall in the uncertainty range resulting from the abundance analysis. Only for HD 46375 do the different indicators give different results.

7. Reanalysis of published *EW* data

Several recent studies have presented measurements of N I lines in targets with known planets (Gonzalez & Laws 2000; Gonzalez et al. 2001; Takeda et al. 2001; Sadakane et al. 2002). We have collected all the *EW* values determined in these papers and used them to calculate nitrogen abundances with atmospheric parameters from Santos et al. (2004).

Gonzalez & Laws (2000) and Gonzalez et al. (2001) measured the N I line at 7468 Å, as we did; therefore, we could compare *EW* values in some of the targets that both analyses had in common. Takeda et al. (2001) and Sadakane et al. (2002) used the N I line at 8683 Å, so we were not able to compare our *EW* values with theirs, but only [N/H]. Besides allowing us to carry out a comparison, the literature values added new abundance measures to our data sample.

This reanalysis was carried out in the same way as described in Sect. 3.2. In the case of the N I line at 8683 Å, the solar gf value computed using the equivalent width (7.0 mÅ) measured in the Solar Atlas (Kurucz et al. 1984) was log gf = 0.068. All the *EW* values from the literature, the atmospheric parameters from Santos et al. (2004) and the resulting nitrogen abundances are presented in Table 8. All the results for the targets in common with our data sample are listed in Table 9. We note that the results from different sources are in good agreement. Significant differences exist only for HD 186427, HD 187123 and HD 217107. The [N/H] and [N/Fe] vs. [Fe/H] trends from the literature *EW* values and from our data are represented in Fig. 7. Figure 5 (bottom panel) shows the [N/H] distribution for comparison sample and planet host stars from all the sources. We note that the new values confirm the trends discussed in the previous sections (see Sect. 4).

8. Discussion and conclusions

In the present study we have determined the nitrogen abundances in 51 planet host stars and in 25 stars from a comparison sample with no known planetary mass companion. Among the set of planet hosts, 28 targets have been analysed by spectral synthesis of the NH band at 3360 Å, while *EW* measurements of the N I 7468.27 Å line were carried out for 31 stars. Another 15 planet hosts were subsequently added to our study, with *EW* values taken from other authors' works. Moreover, we were able to check that the different indicators are in remarkable agreement for several common targets. This result is an independent and homogeneous analysis of nitrogen abundances in 91 solar-type dwarfs, 66 with planets and 25 from a volume-limited comparison sample.

The behaviour of volatiles in planet-harbouring stars with regard to a comparison sample can be very informative for checking the "self-enrichment" hypothesis. If the accretion of metal-enriched planetary material were a key parameter for the observed enhancement of iron abundances, then volatile abundances in planet host stars would not show as much overabundance as refractories do since elements with a lower condensation temperature are expected to be deficient in accreted materials. In that case, the following trend would be observed in planet host stars: [N/H] < [Fe/H].

Table 6. Nitrogen abundances from N I 7468.27 Å for a set of stars with planets and brown dwarf companions.

Star	$T_{\rm eff}$ (K)	$\log g$ (cm s^{-2})	ξ_t (km s^{-1})	[Fe/H]	EW (mÅ)	[N/H]
HD 12661	5702 ± 36	4.33 ± 0.08	1.05 ± 0.04	0.36 ± 0.05	8.5 ± 1	0.35 ± 0.07
HD 16141	5801 ± 30	4.22 ± 0.12	1.34 ± 0.04	0.15 ± 0.04	5.6 ± 1	0.03 ± 0.10
HD 19994	6290 ± 58	4.31 ± 0.13	1.63 ± 0.12	0.24 ± 0.07	13.0 ± 2	0.17 ± 0.09
HD 23596	6108 ± 36	4.25 ± 0.10	1.30 ± 0.05	0.31 ± 0.05	12.6 ± 2	0.22 ± 0.10
HD 30177	5584 ± 65	4.23 ± 0.13	1.14 ± 0.07	0.38 ± 0.09	9.0 ± 2	0.47 ± 0.10
HD 40979	6145 ± 42	4.31 ± 0.15	1.29 ± 0.09	0.21 ± 0.05	10.0 ± 3	0.10 ± 0.16
HD 46375	5268 ± 55	4.41 ± 0.16	0.97 ± 0.06	0.20 ± 0.06	4.0 ± 1	0.42 ± 0.15
HD 50554	6026 ± 30	4.41 ± 0.13	1.11 ± 0.06	0.01 ± 0.04	7.0 ± 1	0.06 ± 0.08
HD 65216	5666 ± 31	4.53 ± 0.09	1.06 ± 0.05	−0.12 ± 0.04	3.0 ± 1	$-0.03^{+0.15}_{-0.19}$
HD 68988	5988 ± 52	4.45 ± 0.15	1.25 ± 0.08	0.36 ± 0.06	13.0 ± 3	0.39 ± 0.15
HD 72659	5995 ± 45	4.30 ± 0.07	1.42 ± 0.09	0.03 ± 0.06	7.0 ± 2	0.04 ± 0.16
HD 73256	5518 ± 49	4.42 ± 0.12	1.22 ± 0.06	0.26 ± 0.06	5.0 ± 1	0.27 ± 0.11
HD 73526	5699 ± 49	4.27 ± 0.12	1.26 ± 0.06	0.27 ± 0.06	7.5 ± 2	0.23 ± 0.16
HD 75732	5279 ± 62	4.37 ± 0.18	0.98 ± 0.07	0.33 ± 0.07	6.5 ± 1	0.65 ± 0.11
HD 76700	5737 ± 34	4.25 ± 0.14	1.18 ± 0.04	0.41 ± 0.05	9.0 ± 2	0.32 ± 0.14
HD 80606	5574 ± 72	4.46 ± 0.20	1.14 ± 0.09	0.32 ± 0.09	7.5 ± 2	0.44 ± 0.17
HD 95128	5954 ± 25	4.44 ± 0.10	1.30 ± 0.04	0.06 ± 0.03	6.4 ± 2	0.06 ± 0.16
HD 120136	6339 ± 73	4.19 ± 0.10	1.70 ± 0.16	0.23 ± 0.07	16.2 ± 2	0.19 ± 0.09
HD 134987	5776 ± 29	4.36 ± 0.07	1.09 ± 0.04	0.30 ± 0.04	10.0 ± 2	0.39 ± 0.12
HD 142415	6045 ± 44	4.53 ± 0.08	1.12 ± 0.07	0.21 ± 0.05	10.0 ± 2	0.24 ± 0.13
HD 143761	5853 ± 25	4.41 ± 0.15	1.35 ± 0.07	−0.21 ± 0.04	2.5 ± 1	$-0.29^{+0.17}_{-0.25}$
HD 145675	5311 ± 87	4.42 ± 0.18	0.92 ± 0.10	0.43 ± 0.08	5.3 ± 2	0.50 ± 0.19
HD 168443	5617 ± 35	4.22 ± 0.05	1.21 ± 0.05	0.06 ± 0.05	6.0 ± 3	$0.24^{+0.23}_{-0.36}$
HD 178911B	5600 ± 42	4.44 ± 0.08	0.95 ± 0.05	0.27 ± 0.05	8.0 ± 2	0.46 ± 0.17
HD 186427	5772 ± 25	4.40 ± 0.07	1.07 ± 0.04	0.08 ± 0.04	3.4 ± 1	−0.13 ± 0.14
HD 187123	5845 ± 22	4.42 ± 0.07	1.10 ± 0.03	0.13 ± 0.03	6.1 ± 2	0.11 ± 0.16
HD 190360	5584 ± 36	4.37 ± 0.06	1.07 ± 0.05	0.24 ± 0.05	6.3 ± 2	0.32 ± 0.16
HD 216770	5423 ± 41	4.40 ± 0.13	1.01 ± 0.05	0.26 ± 0.04	7.0 ± 2	0.54 ± 0.19
HD 217107	5663 ± 36	4.34 ± 0.08	1.11 ± 0.04	0.37 ± 0.05	8.7 ± 1	0.28 ± 0.06
HD 219542B	5732 ± 31	4.40 ± 0.05	0.99 ± 0.04	0.17 ± 0.04	8.0 ± 1	0.39 ± 0.13
HD 222582	5843 ± 38	4.45 ± 0.07	1.03 ± 0.06	0.05 ± 0.05	6.0 ± 2	0.12 ± 0.16

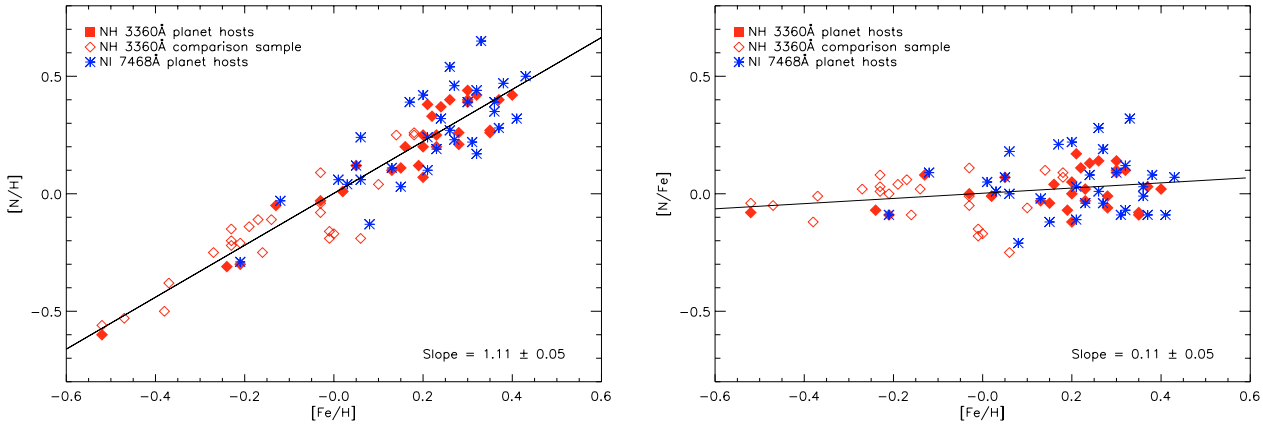

Fig. 6. [N/H] and [N/Fe] vs. [Fe/H] plots from NH 3360 Å band and N I 7468 Å line values. Filled diamonds and open diamonds represent planet host and comparison sample stars from NH band synthesis, respectively, while asterisks denote planet host stars from N I line analysis. Linear least-squares fits to all samples together are represented and slope values are written at the bottom of each plot.

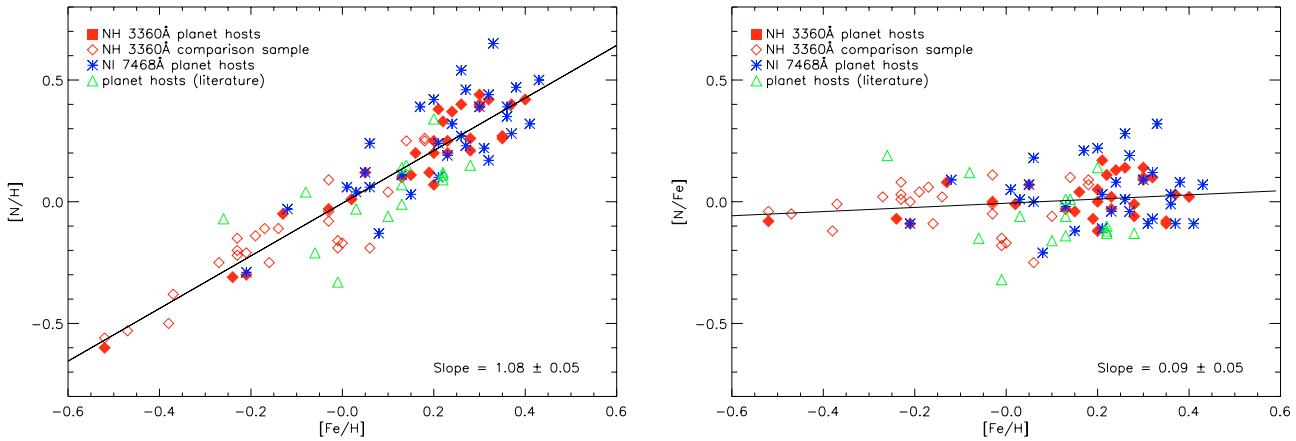

Fig. 7. [N/H] and [N/Fe] vs. [Fe/H] plots from NH 3360 Å band, N I 7468 Å line and literature values. Filled and open diamonds represent planet host and comparison sample stars from NH band synthesis, respectively. Asterisks and open triangles denote planet host stars from N I line and from literature values, respectively. Linear least-squares fits to all samples together are represented and slope values are written at the bottom of each plot.

Our results suggest that planet hosts stars do not behave in such a way. The [N/H] abundance scales with that of the iron. In the [N/Fe] vs. [Fe/H] plots, no significant trace of [N/Fe] < 0 appears in stars with planets. Moreover, planet host and comparison sample stars have the same behaviour. Trends from either sample are quite indistinguishable. This emphasizes that the trend predicted from the "self-enrichment" scenario is not observed at all.

Previous studies have obtained similar results for other volatiles in some planet-harbouring stars. Gonzalez et al. (2001) corrected the low [C/Fe] values found in a previous study (Gonzalez & Laws 2000) and concluded that [C/Fe] and [O/Fe] in planet hosts do not display significant differences from those in field dwarfs of the same [Fe/H]. Takeda et al. (2001) found the same trend as we did for N, C, S, O and Zn in 14 planet hosts, and in Sadakane et al. (2002) this result was confirmed for C and O in another 12 planet-harbouring stars. Our study confirms these results for a significantly larger set of stars with planets, as well as in a comparison sample of stars with no discovered planetary-mass companion. This seems to support a scenario in which the formation of planets is particularly dependent on the high metallicity of the primordial cloud.

In the future, it will be important to pursue further uniform studies of volatile element (C, O, S and Zn) abundances in planet hosts and stars with no known planets. Well-defined [*X*/Fe] vs. [Fe/H] distributions can provide us with precise information in order to confirm or discard hypotheses about planetary formation.

Another important piece of information that emerges from nitrogen abundance trends concerns nitrogen sources. The latest studies propose two sources of primary nitrogen: intermediate mass (4–8 $M_{\odot}$) and massive stars ($M > 8\ M_{\odot}$). If the latter source were the main contributor to nitrogen at high [Fe/H], N and Fe abundances would appear to be uncoupled and nitrogen would be overabundant relative to iron. Our study of nitrogen abundances in 91 solar-type dwarfs suggests that nitrogen keeps pace with iron. The [N/H] vs. [Fe/H] plots show that the two elements behave quite similarly, and the

Table 7. Comparison of nitrogen abundances determined from NH band synthesis and from N I line analysis.

Star	$[N/H]_{NH\,3360}$	$[N/H]_{N\,I\,7468}$
HD 16141	0.11	0.03
HD 19994	0.37	0.17
HD 46375	0.07	0.42
HD 120136	0.20	0.19
HD 134987	0.40	0.39
HD 143761	−0.30	−0.29
HD 217107	0.40	0.28
HD 222582	0.12	0.12

[N/Fe] vs. [Fe/H] plots indicate that no significant nitrogen overabundance exists relative to iron in the metallicity range −0.6 < [Fe/H] < +0.4. We also note that Shi et al. (2002) recently obtained that [N/Fe] is about solar in a sample of 90 disk stars; therefore, they concluded that nitrogen is produced mostly by intermediate mass stars.

Nevertheless, secondary production due to ILMS is the predominant effect on the [N/Fe] curve around solar metallicities. Only the [N/Fe] trend at [Fe/H] < −1.0 can provide conclusive arguments about primary sources. At this time, we are extending our study of [N/H] ratios to lower metallicities, by applying the same analysis of the NH band at 3360 Å to a sample of metal-poor dwarfs. The results will be very informative in the framework of investigating the sources of primary nitrogen in the early Galaxy.

Acknowledgements. We would like to thank J. I. González Hernández for kindly providing us with his program FITTING. We wish to thank Dr. G. Meynet (Observatoire de Genève, Switzerland) for many fruitful discussions and his comments on the text. The anonymous referee is thanked for many useful suggestions and comments. IRAF is distributed by the National Optical Astronomy Observatories, operated by the Association of Universities for Research in Astronomy, Inc., under contract with the National Science Foundation, USA.

Table 8. Nitrogen abundances calculated using *EW* values from other authors for a set of stars with planets and brown dwarf companions.

Star	Ref.	$T_{\rm eff}$ (K)	$\log g$ (cm s^{-2})	ξ_t (km s^{-1})	[Fe/H]	*EW* (mÅ)	[N/H]
HD 75289	1	6143 ± 53	4.42 ± 0.13	1.53 ± 0.09	0.28 ± 0.07	10.7	0.15
HD 9826	1	6212 ± 64	4.26 ± 0.13	1.69 ± 0.16	0.13 ± 0.08	9.2	−0.01
HD 9826	3	6212 ± 64	4.26 ± 0.13	1.69 ± 0.16	0.13 ± 0.08	19.6	0.14
HD 9826	avg.	6212 ± 64	4.26 ± 0.13	1.69 ± 0.16	0.13 ± 0.08	–	0.07
HD 10697	2	5641 ± 28	4.05 ± 0.05	1.13 ± 0.03	0.14 ± 0.04	6.0	0.15
HD 89744	2	6234 ± 45	3.98 ± 0.05	1.62 ± 0.08	0.22 ± 0.05	13.3	0.09
HD 89744	3	6234 ± 45	3.98 ± 0.05	1.62 ± 0.08	0.22 ± 0.05	22.9	0.12
HD 89744	avg.	6234 ± 45	3.98 ± 0.05	1.62 ± 0.08	0.22 ± 0.05	–	0.11
HD 217014	2	5804 ± 36	4.42 ± 0.07	1.20 ± 0.05	0.20 ± 0.05	9.0	0.34
HD 117176	3	5560 ± 34	4.07 ± 0.05	1.18 ± 0.05	−0.06 ± 0.05	4.0	−0.21
HD 106252	4	5899 ± 35	4.34 ± 0.07	1.08 ± 0.06	−0.01 ± 0.05	4.9	−0.33
HD 134987	2	5776 ± 29	4.36 ± 0.07	1.09 ± 0.04	0.30 ± 0.04	10.6	0.43
HD 143761	3	5853 ± 25	4.41 ± 0.15	1.35 ± 0.07	−0.21 ± 0.04	6.1	−0.12
HD 168443	2	5617 ± 35	4.22 ± 0.05	1.21 ± 0.05	0.06 ± 0.05	4.8	0.12
HD 186427	3	5772 ± 25	4.40 ± 0.07	1.07 ± 0.04	0.08 ± 0.04	10.8	0.22
HD 187123	4	5845 ± 22	4.42 ± 0.07	1.10 ± 0.03	0.13 ± 0.03	6.5	−0.14
HD 95128	3	5954 ± 25	4.44 ± 0.10	1.30 ± 0.04	0.06 ± 0.03	13.0	0.18
HD 12661	2	5702 ± 36	4.33 ± 0.08	1.05 ± 0.04	0.36 ± 0.05	9.0	0.38
HD 217107	2	5663 ± 36	4.34 ± 0.08	1.11 ± 0.04	0.37 ± 0.05	3.9	−0.03
HD 222582	2	5843 ± 38	4.45 ± 0.07	1.03 ± 0.06	0.05 ± 0.05	4.9	0.02
HD 75732	3	5279 ± 62	4.37 ± 0.18	0.98 ± 0.07	0.33 ± 0.07	10.5	0.70
HD 120136	1	6339 ± 73	4.19 ± 0.10	1.70 ± 0.16	0.23 ± 0.07	16.7	0.21
HD 130322	4	5392 ± 36	4.48 ± 0.06	0.85 ± 0.05	0.03 ± 0.04	3.2	−0.03
HD 141937	4	5909 ± 39	4.51 ± 0.08	1.13 ± 0.06	0.10 ± 0.05	7.7	−0.06
HD 168746	4	5601 ± 33	4.41 ± 0.12	0.99 ± 0.05	−0.08 ± 0.05	5.6	0.04
HD 190228	4	5327 ± 35	3.90 ± 0.07	1.11 ± 0.05	−0.26 ± 0.06	3.5	−0.07

Ref. 1 from Gonzalez & Laws (2000).
Ref. 2 from Gonzalez et al. (2001).
Ref. 3 from Takeda et al. (2001).
Ref. 4 from Sadakane et al. (2002).

Table 9. Comparison of nitrogen abundances determined using *EW* values (in mÅ) from our data and from other authors.

Star	$T_{\rm eff}$ (K)	$\log g$ (cm s^{-2})	ξ_t (km s^{-1})	[Fe/H]	EW^1 7468	EW^2 7468	EW^3 8683	[N/H]^1	[N/H]^2	[N/H]^3
HD 134987	5776	4.36	1.09	0.30	10.0	10.6	–	0.39	0.43	–
HD 143761	5853	4.41	1.35	−0.21	2.5	–	6.1	−0.29	–	−0.12
HD 168443	5617	4.22	1.21	0.06	6.0	4.8	–	0.24	0.12	–
HD 186427	5772	4.40	1.07	0.08	3.4	–	10.8	−0.13	–	0.22
HD 187123	5845	4.42	1.10	0.13	6.1	–	6.5	0.11	–	−0.14
HD 95128	5954	4.44	1.30	0.06	6.4	–	13.0	0.06	–	0.18
HD 12661	5702	4.33	1.05	0.36	8.5	9.0	–	0.35	0.38	–
HD 217107	5663	4.34	1.11	0.37	8.7	3.9	–	0.28	−0.03	–
HD 222582	5843	4.45	1.03	0.05	6.0	4.9	–	0.12	0.02	–
HD 75732	5279	4.37	0.98	0.33	6.5	–	10.5	0.65	–	0.70
HD 120136	6339	4.19	1.70	0.23	16.2	16.7	–	0.19	0.21	–

[1] *EW* values from our data.
[2] *EW* values from Gonzalez & Laws (2000) and Gonzalez et al. (2001).
[3] *EW* values from Takeda et al. (2001) and Sadakane et al. (2002).

References

Anders, E., & Grevesse, N. 1989, Geochim. Cosmochim. Acta, 53, 197

Bensby, T., Feltzing, S., & Lundström, I. 2003, A&A, 410, 527

Bessel, M. S., & Norris, J. 1982, ApJ, 263, L29

Bodaghee, A., Santos, N. C., Israelian, G., & Mayor, M. 2003, A&A, 404, 715

Carbon, D. F., Barbuy, B., Kraft, R. P., Friel, E. D., & Suntzeff, N. B. 1987, PASP, 99, 335

Edvardsson, B., Andersen, J., Gustafsson, B., et al. 1993, A&A, 275, 101

Gray, D. 1992, in The observation and analysis of stellar photospheres (Cambridge Univ. Press)

Grevesse, N., Lambert, D. L., Sauval, A. J., et al. 1990, A&A, 232, 225

Gonzalez, G., & Laws, C. 2000, AJ, 119, 390

Gonzalez, G., Laws, C., Tyagi, S., & Reddy, B. E. 2001, AJ, 121, 432

Henry, R. B. C., Edmunds, M. G., & Koppen, J. 2000, ApJ, 541, 660

Israelian, G., Santos, N. C., Mayor, M., & Rebolo, R. 2001, Nature, 411, 163

Israelian, G., Santos, N. C., Mayor, M., & Rebolo, R. 2003, A&A, 405, 753

Israelian, G., Santos, N. C., Mayor, M., & Rebolo, R. 2004, A&A, 414, 601

Izotov, Y. I., & Thuan, T. X. 2000, New Astr. Rev., 44, 329

Kurucz, R. L. 1993, CD-ROMs, ATLAS9 Stellar Atmospheres Programs and 2 km s^{-1} Grid (Cambridge: Smithsonian Astrophys. Obs.)

Kurucz, R. L., Furenlid, I., Brault, J., & Testerman, L. 1984, Solar Flux Atlas from 296 to 1300 nm, NOAO Atlas No. 1

Laird, J. B. 1985, ApJ, 289, 556

Liang, Y. C., Zhao, G., & Shi, R. J. 2001, A&A, 374, 936

Maeder, A. & Meynet, G. 2000, ARA&A, 38, 143

Marigo, P. 2001, A&A, 370, 194

Meynet, G., & Maeder, A. 2002, A&A, 390, 561

Moore, C. E., Minnaert, M. G. J., & Houtgast, J. 1966, The Solar Spectrum 2934 Å to 8770 Å

Pagel, B. E. J., & Edmunds, M. G. 1981, ARA&A, 19, 77

Pettini, M., Ellison, S. L., Bergeron, J., & Petitjean, P. 2002, A&A, 391, 21

Pinsonneault, M. H., DePoy, D. L., & Coffee, M. 2001, ApJ, 556, L59

Sadakane, K., Ohkubo, Y., Takeda, Y., et al. 2002, PASJ, 54, 911

Santos, N. C., Israelian, G., & Mayor, M. 2000, A&A, 363, 228

Santos, N. C., Israelian, G., & Mayor, M. 2001, A&A, 373, 1019

Santos, N. C., García López, R. J., Israelian, G., et al. 2002, A&A, 386, 1028

Santos, N. C., Israelian, G., Mayor, M., Rebolo, R., & Udry, S. 2003, A&A, 398, 363

Santos, N. C., Israelian, G., & Mayor, M. 2004, A&A, 415, 1153

Smith, V. V., Cunha, K., & Lazzaro, D. 2001, AJ, 121, 3207

Sneden, C. 1973, Ph.D. Thesis, University of Texas

Shi, J. R., Zhao, G., & Chen, Y. Q. 2002, A&A, 381, 982

Takeda, Y., Sato, B., Kambe, E., et al. 2001, PASJ, 53, 1211

Tomkin, J., & Lambert, L. 1984, ApJ, 279, 220

van den Hoek, L. B., & Groenewegen, M. A. T. 1997, A&AS, 123, 305

Yakovina, L. A., & Pavlenko, Ya. V. 1998, Kinematics and Physics of Celestial Bodies, 14, 195